The flocculation state of mud in the lowermost freshwater reaches of the Mississippi River: spatial distribution of sizes, seasonal changes, and their impact on vertical concentration profiles

Ryan Osborn[1,4], Kieran B.J. Dunne[2], Thomas Ashley[1], Jeffrey A. Nittrouer[3], and Kyle Strom[1]

[1]Civil and Environmental Engineering, Virginia Tech, Blacksburg VA USA
[2]Caltech, Division of Geological and Planetary Sciences, Pasadena, CA, USA
[3]Texas Tech University, Department of Geosciences, Lubbock, TX, USA
[4]Now at United States Department of Agriculture, Natural Resources Conservation Service, Boise, ID, USA

Key Points:

- Mud in the Mississippi is flocculated in freshwater reaches, and floc sizes change little in the lateral or vertical direction at a station
- All else being equal, flocs are larger during the summer than they are during the winter
- Measured floc sizes can easily explain stratification in mud concentration profiles in some, but not all, instances

Corresponding author: Kyle Strom, `strom@vt.edu`

Abstract

We use in situ measurements of suspended mud to assess the flocculation state of the lowermost freshwater reaches of the Mississippi River. The goal of the study was to assess the flocculation state of the mud in the absence of seawater, the spatial distribution of floc sizes within the river, and to look for seasonal differences between summer and winter. The data was also used to examine whether measured floc sizes could explain observed vertical distributions of suspended sediment concentration through a Rouse profile analysis. The surveys were conducted at the same location during summer and winter at similar discharges and suspended sediment concentrations, and in situ measures of the size distribution of the mud over the longitudinal, transverse, and vertical directions within the river were obtained using a specially developed underwater imaging system. These novel observations show that mud in the Mississippi is flocculated with median floc sizes ranging from 50 to 200 microns depending on location and season. On average flocs were found to be 40 microns larger during summer than in winter and to slightly increase in size moving downriver from the Bonnet Carré Spillway to Venice, LA. Floc size statistics varied little over the depth or laterally across the river at a given station. Bulk settling velocities calculated from size measurements matched values obtained from a Rouse profile analysis at stations with sandy beds, but underestimated settling velocities using the same equation parameters for measurements made during winter over muddy beds.

Plain Language Summary

Rivers such as the Mississippi carry a significant amount of fine muddy sediment. Where this mud deposits, be it within the river channel itself, the river's floodplains, or the coastal zone depends in part on how fast the mud particles settle within the water. Muddy sediment can exist as a collection of individual particles ranging in size from 1 to 63 microns and/or as aggregates of these particles, known as flocs, whose size, density, and settling velocity change with physical, chemical, and biological conditions within the water column. Whether mud exists as flocs and how big the flocs are if they do exist in different conditions within a river is difficult to know. The challenges come from the dynamic nature of the aggregate sizes and the difficulty in measuring these flocs within the river itself. In this study, we present data, for the first time, on the flocculation state of mud in the lower freshwater sections of the Mississippi River. Such data aids in understanding where mud may travel to and deposit within the lower Mississippi River Delta and whether or not engineering solutions to land loss such as diversion structures can help to promote the emergence of new land.

1 Introduction

Fine muddy sediment with grain sizes less than 63 μm in diameter constitutes a significant fraction of the total sediment load carried by lowland rivers. For example, over the three flood years of 2008-2010, Allison et al. (2012) estimated that 70% of the total sediment load passing Baton Rouge, LA, and over 90% exiting to the Gulf of Mexico was mud. A unique attribute of muddy sediment is its potential to form flocs or aggregates of particles that can change in size, density, and hence settling velocity depending on turbulence conditions in the flow, the amount and type of available sediment, water chemistry, and the level of available organic material and microbial activity (Eisma, 1986; Mietta et al., 2009; Verney et al., 2009; Lefebvre et al., 2012; Horemans et al., 2021; Deng et al., 2021). From a sediment transport perspective, the flocculation potential of mud is significant because particle settling velocity, in conjunction with local concentration, sets sediment deposition rates and can influence the average transport hop length of the suspended material.

Research into the flocculation behavior of muds, and the impact of flocs on sediment transport dynamics, has primarily been investigated within the context of saline coastal and estuarine environments (Kranck, 1973; Gibbs, 1985; Eisma, 1986; Kranck & Milligan, 1992; A. Manning & Dyer, 2002). Salt is known to enhance flocculation in laboratory studies of settling in a stagnant column (Kranck, 1980; Kim & Nestmann, 2009), and is often thought to be a controlling factor on flocculation in the field due to the large accumulations of mud in estuarine conditions where fresh and saltwater mix and the reduction in the thickness of the electric double layer is known to occur in the presence of cations (Tan et al., 2013); this is true even though many have pointed to organic binders as possibly being the major factor contributing to flocculation of mud in saltwater conditions (e.g., Eisma, 1986; Verney et al., 2009), and hydrodynamic, rather than salt, being responsible for mud accumulations (e.g., Thill et al., 2001). Nevertheless, the flocculation of mud is known to exert a strong control on mud dynamics in coastal environments.

Comparatively fewer studies have sought to measure floc properties in freshwater settings or to assess the contribution of flocs to sediment transport dynamics in rivers. The primary reason for this is that mud flocs in freshwater have historically been assumed to be nonexistent or too small to significantly impact river morphology. Conventional wisdom has considered mud concentration as being uniformly distributed over the depth, due to fluid shear velocity in most rivers being significantly higher than the settling velocity of unflocculated mud (i.e., Rouse numbers < 0.01). Hence, this washload sediment has been thought to be prohibited from depositing on the bed. This consideration has two important implications: (1) riverine mud does not contribute to buoyancy-induced turbulence damping because vertical concentration gradients do not exist (Wright & Parker, 2004b), and (2) mud moves through the fluvial system as washload exerting little morphologic influence (Biedenharn et al., 2000).

Despite the lingering traditional view of fluvial mud, there is significant evidence that mud does exist in aggregate or flocculated form in freshwater fluvial systems. Microscope imaging of sediment captured from freshwater rivers at low (Le et al., 2020), mid (Droppo & Ongley, 1994; Fox et al., 2013), and high latitudes (Droppo et al., 1998) all suggest that material in suspension, and on the bed, are indeed flocculated even in the absence of typical oceanic or estuarine levels of salinity. Various sizing and settling estimates of mud within freshwater suspensions also all point to mud existing in some state of aggregation in freshwater systems (Phillips & Walling, 1999; Bungartz et al., 2006; Woodward & Walling, 2007; Marttila & Kløve, 2015). Furthermore, recent analyses of vertical concentration profiles of mud for many rivers worldwide have shown that mud can indeed be vertically stratified and that flocculation could provide an explanation for the observed behavior (Lamb et al., 2020; Izquierdo-Ayala et al., 2021; Nghiem et al., 2022).

Unlike estuarine sampling where flocs have been imaged and sized in situ with specially designed camera systems (e.g., Fennessy et al., 1994; A. J. Manning & Dyer, 2002; Cartwright et al., 2011; Markussen et al., 2016; Fall et al., 2021), the observation of freshwater aggregates has largely been accomplished through laboratory microscope analysis of samples collected from the water column or bed at some earlier point in time. While this method is not ideal when an understanding of the impact of flocs on sediment transport is desired, it does provide the opportunity to study the composition of the flocs in detail. Such analysis of river water samples shows a significant presence of particle aggregates or flocs, and that the flocs are similar in shape and composition to those found in estuaries (Droppo & Ongley, 1994; Fox et al., 2013; Spencer et al., 2021), though they tend to be of size < 100 μm. Similar to those in estuaries, freshwater flocs are composed of complex assemblages of inorganic clays and silts, organic detrital material, and particle-attached bacteria and their polymeric byproducts (Liss et al., 1996; Droppo et al., 1997; Fall et al., 2021). In the absence of salt then, it is commonly held that these biofilms and biofilm components are the binding mechanisms for floc assemblages in freshwater settings.

If freshwater flocs are bound together by various organic constituents, then one might expect seasonal or condition-dependent changes in nutrients, temperature, or organic content, in addition to physical conditions such as turbulence or suspended sediment concentration, to influence floc characteristics. Data are lacking to fully define the nature of freshwater flocs under different physical, chemical, and biological conditions. However, a few studies have indeed observed seasonal or condition-dependent changes in freshwater aggregates' size or shape, and all of them point to some type of alteration in the organics as the underlying driver of the change. For example, Phillips and Walling (1999) observe that mud aggregate size was largest during the spring and summer and that the timing of the observed peak in aggregate size corresponded with the peak in organic content within the bed. Relatedly, Fox et al. (2013) found that aggregates were more irregular and elongated in summer compared to more compact and spherical aggregates in the fall and that the changes in aggregate morphology were highly correlated with seasonal changes in heterotrophic and autotrophic biological activity within the mud deposited on the stream bed. Changes in organic material type within the water column have also been linked to differences in the potential of the system to generate flocs. For example, Lee et al. (2017) and Lee et al. (2019) found that rain-driven high flows lead to an increase in organic content rich in terrestrial humic substances in the Nakdong River in Korea. However, the humic-substance-based organics were observed to have a stabilizing effect on the suspended particles thereby suppressing flocculation. Whereas low-flow conditions led to warmer water, algae growth, and associated extracellular polymeric substances (EPS) which enhanced the potential of the water to promote flocculation. Seasonality in estuarine floc sizes or settling properties have also been linked to changes in organic and mineral constituents of the suspension throughout the year (Van der Lee, 2000; Mikkelsen et al., 2007; Verney et al., 2009; Fettweis & Baeye, 2015; Deng et al., 2021; Fettweis et al., 2022).

Identification of flocs in freshwater systems has mostly come through either microscope analysis of aggregates obtained from water column grab or pumped samples or through an indirect measure of size through estimates of settling velocity from a Rouse profile analysis of suspended sediment concentration. In the case of microscope imaging, the material is imaged in conditions different from those the material experienced in its natural setting. This is significant because flocs have the ability to change their size as the shearing and mixing level of the fluid changes, e.g., going from the river to a sample bottle or sampling pipette to a slide. Furthermore, if the material is allowed to settle, it is easier for material to aggregate in the zones of higher sediment concentrations experienced at the bottom of a sampling container from which material might be extracted for imaging. Therefore it is possible that flocs imaged in the lab from field water column samples might not be completely representative of the flocs as they exist within the turbulent flow of the river. In addition, the fraction of the mud that exists as flocs, the distribution of floc sizes within the river, and whether or not the flocs themselves influence mud transport in a geomorphically meaningful sense is still unclear. For example, the studies of (Lamb et al., 2020) and (Nghiem et al., 2022) provide compelling evidence that flocculation of the mud is a reasonable explanation for the existence of vertical gradients in mud concentration profiles observed in rivers, and the average settling velocities needed to produce such observed gradients are large enough to expect flocs to play a significant role in the rivers morphology. Yet, the concentration data used in these studies was not paired with in situ size measurements of the mud, and a direct link between flocculation state river morphology has yet to be made.

In this field study, we provide in situ size observations of the suspended mud and sand in the freshwater reaches of the main channel of the Mississippi River before it enters terminal distributaries and embayments. The specific questions we seek to answer with the data are: (1) does mud exist in flocculated form during moderately high flows in the freshwater reaches of the lower Mississippi River; (2) if so, how are floc sizes distributed over the vertical (depth), lateral (right to left bank), and longitudinal (up and downstream river stations with slightly different hydraulic conditions); (3) are there any seasonal differences in observed flocs between summer and winter; and (4) can measured floc sizes explain measured vertical gradients of mud concentration? To explore these questions, we used the imaging system of Osborn et al. (2021) to obtain direct observations of suspended sediment over the water column during a summer and winter survey in the Mississippi River.

2 Methods

2.1 Overview

The primary data needed to explore our research questions include: in situ measurements of particle and/or floc sizes over the vertical at each sampling location in the river, water column samples of suspended sediment, samples of the bed sediment, and the velocity distribution and shear velocity at the location where profiles of floc size and concentration are measured. Comparison of the data obtained from these samples at different spatial locations, and comparisons between the summer and winter surveys, provide the basis for investigating the flocculation state of mud in the river with respect to location and season (research questions 1-3). Question 4 is investigated by comparing the settling velocity of the mud flocs calculated from the measured floc sizes to the settling velocity obtained by fitting a Rouse concentration profile to the measured concentration data.

2.2 Background theory: the Rouse profile

The Rouse profile (Rouse, 1939) is a particular solution to the following simplified advection-diffusion equation for suspended particulate load,

$$w_s C + \epsilon_s \frac{dC}{dz} = 0 \tag{1}$$

Here C is the suspended sediment concentration, z is the vertical coordinate, and ϵ_s is the vertical sediment diffusivity coefficient used in conjunction with the vertical gradient of C to model vertical advective flux due to time-averaged turbulence. Equation 1 assumes equilibrium transport conditions, i.e., that C is locally steady, that velocity and concentration in the down and cross-stream directions are uniform, and that there is no net sediment flux across the free surface. A result of these conditions is that the downward flux of sediment due to settling ($-w_s C$) must be balanced with the upward turbulent diffusive flux ($\epsilon_s dC/dz$).

The Rouse profile solution to equation 1 uses a model for ϵ_s based on the 2D shear stress distribution, i.e., $\tau = \rho u_*^2(1 - z/H)$ (where ρ is the fluid density, u_* is the shear velocity, and H is the total flow depth), and the argument that suspended sediment diffuses as a result of the eddying motions that also lead to the diffusion of fluid momentum, $\epsilon_s = \nu_T/\beta$, where ν_T is the eddy viscosity or diffusion rate of momentum and β is the Schmidt number which accounts for any differences between mass and momentum diffusion rates. To provide closure, Prandtl's mixing length theory and the resulting rough-wall log law,

$$\frac{u}{u_*} = \frac{1}{\kappa} \ln \left(30 \frac{z}{k_c} \right) \tag{2}$$

can be used in conjunction with the Boussinesq hypotheses, $\tau = \nu_T(du/dz)$, to yield the following equation for ϵ_s:

$$\epsilon_s = \frac{1}{\beta} \kappa u_* z \left(1 - \frac{z}{H}\right) \tag{3}$$

In equation 2, u is the depth-varying and time-averaged velocity, κ is the von Kàrman constant, and k_c is a composite bed roughness length scale. To account for damping of turbulence due to vertical density stratification, the effective eddy viscosity can be conceived of as the product of the neutral, unstratified eddy viscosity, ν_{T0}, and a factor γ that ranges from $\gamma = 1$ for unstratified conditions to 0 for complete damping, $\nu_T = \gamma\nu_{T0}$. Making use of γ, equation 3 becomes:

$$\epsilon_s = \frac{\gamma}{\beta}\kappa u_* z \left(1 - \frac{z}{H}\right) \tag{4}$$

Using equation 4 in the integration of equation 1 gives rise to the well-known Rouse concentration profile:

$$\frac{C}{C_b} = \left[\frac{(z/H-1)b}{(b/H-1)z}\right]^{Z_R} \tag{5}$$

with b being a reference height above the bed (often taken at $z/H = 0.05$), and C_b being the concentration at that reference height, $C(z = b) = C_b$. The exponent Z_R is defined as the Rouse number:

$$Z_R = \frac{\beta w_s}{\gamma\kappa u_*} \tag{6}$$

The Rouse number represents a ratio of downward settling velocity to upward turbulent diffusion velocity of the sediment captured by the ratio of w_s/u_*; the three parameters of γ, β, and κ all represent modifiers on u_* to make it a suitable velocity scale for upward diffusion of sediment due to turbulence. Often β is taken as 1 and $\kappa = 0.41$. γ is also often taken as 1 for simplicity, but it can also be set through additional closure equations to account for vertical damping of turbulence in the presence of density stratification.

For large, low-sloping sand-bed rivers, such as the Mississippi, Wright and Parker (2004a) took the approach of defining a single modifier, α, to account for deviation in the baseline case of $\beta = 1$ and $\gamma = 1$ that could be caused by sediment induced stratification. In their model, α is equal to γ/β and hence the Rouse number is defined as:

$$Z_R = \frac{w_s}{\alpha\kappa u_*} \tag{7}$$

with α provided through the following empirical fit,

$$\alpha = \begin{cases} 1 - 0.06\left(\frac{C_{5t}}{S_0}\right)^{0.77} & \text{for } \frac{C_{5t}}{S_0} \leq 10 \\ 0.67 - 0.0025\left(\frac{C_{5t}}{S_0}\right) & \text{for } \frac{C_{5t}}{S_0} > 10 \end{cases} \tag{8}$$

In equation 8, C_{5t} is the volume concentration of suspended sediment at 5% of the flow depth from the bed, and S_0 is the water surface slope. The fit for equation 8 was developed for C_{5t}/S_0 values ranging from 0 to ≈ 50 with the majority of the points falling between 0 and 20.

In our particular study, we are interested in fitting equation 5 to measured mud concentration data for the purpose of obtaining an effective settling velocity for the concentration profile. The data needed to back out a settling velocity estimate in this way includes measures of concentration over the vertical, a measure of the friction velocity, and an estimate of α.

2.3 Survey locations and general river conditions

Data on the flocculation state of the mud, and data for the Rouse profile analysis came from summer and winter sampling surveys. Surveys on the lower Mississippi River were conducted during summer 2020 and winter 2021. Data were collected at several locations within the river and its distributaries during both surveys. However, in this paper, we focus on data only at three key freshwater locations. These stations are, starting from upstream and progressing downstream, the Bonnet Carré Spillway (BCS) (Fig. 1a), the main channel 2 km upriver from the Baptiste Collette distributary, hereinafter referred to as Venice Main Channel (VMC), and at a location within the upstream section of Southwest Pass (SWP) (Fig. 1b). During the summer survey, data were collected at two locations along a lateral transect at the BCS and three locations at VMC. The winter survey consisted of data collection at one location within the thalweg at both the BCS and VMC, and a station located approximately 3 km downriver from Head of Passes with SWP just upstream of a saltwater wedge that was being pushed seaward during the survey.

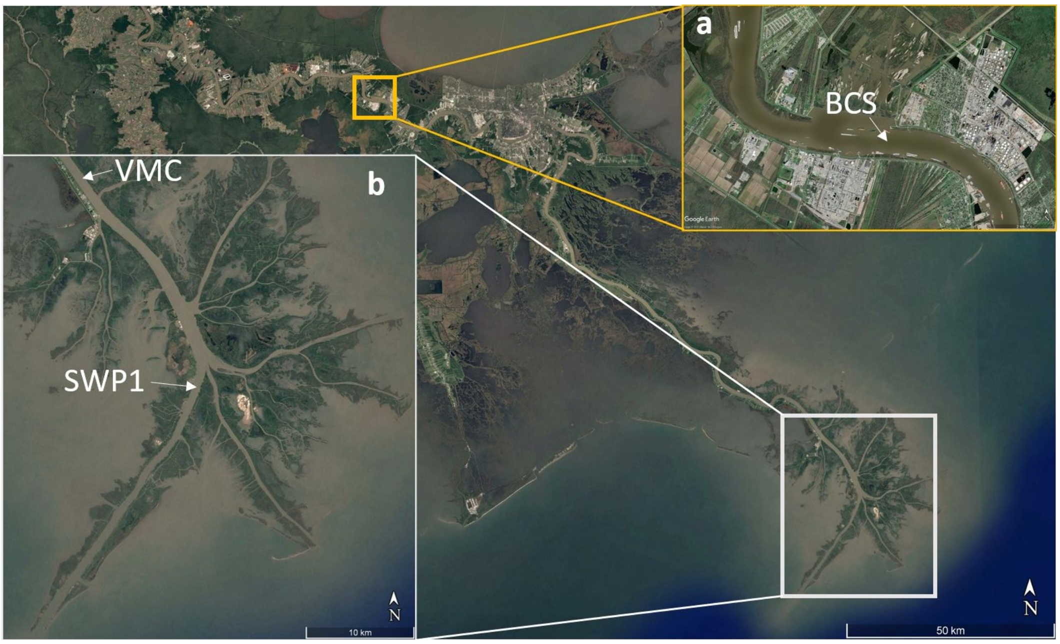

Figure 1. Survey locations. (a) Bonnet Carré Spillway (BCS). (b) Mississippi River Delta, including stations VMC and SWP1.

Contextual discharge, water temperature, and average suspended sediment concentration data for the two surveys were acquired from USGS station 07374000 at Baton Rouge, LA (Table 1). During the summer survey (June 24 - July 2, 2020), the river was on the receding limb of a flow event that reached a peak discharge of just over 28,300 cms before the start of the survey. Over the duration of the summer survey, the discharge dropped from 22,200 cms on June 24 to 16,480 cms on July 2. The average daily water temperature during the summer survey was 27.3 °C. The winter survey took place from January 9-14, 2021. In the five months prior to the survey, discharge did not exceed 13,500 cms. Then, approximately one week before the winter survey, discharge began to increase from 12,000 cms on January 2, 2021, up through the end of the survey period on January 14, 2021. During the survey, discharge ranged from 17,783 cms on January 9 to 19,737 cms on January 14. The daily average water temperature during the winter survey was 6.3 °C.

Average daily turbidity values are reported from the Baton Rouge station. Paired historic USGS physical water column samples of suspended sediment and measured turbidity in FNU were used to create a calibration equation, $C_{avg} = 2.0(\text{FNU}) + 32.4$ ($R^2 = 0.81$), between turbidity and concentration. Using the calibration equation, suspended

Survey Season	Start Date	End Date	Q_{avg} [cms]	Q_{start} [cms]	Q_{end} [cms]	T_{avg} [deg C]	C^*_{avg} [mg/L]
Summer	2020-06-24	2020-07-02	19,073	22,200	16,480	27.3	126
Winter	2021-01-09	2021-01-14	18,939	17,783	19,737	6.3	182

Table 1. Discharge, temperature, and suspended sediment concentration at the USGS 07374000 Baton Rouge station. *obtained through a calibration between USGS measured SSC and FNU.

sediment concentration was between 100 and 200 mg/L during both surveys with concentration being greater during winter (Table 1).

2.4 Field measurements

All sampling and field measurements were made on the river from an 8 m survey vessel. Primary data collected included floc size and concentration measurements over the vertical, water column velocity over the vertical, physical water column samples over the vertical, and bed sediment samples.

Particle and/or floc sizes and concentrations were obtained with the Floc AReA and siZing Instrument (FlocARAZI) imaging system (Osborn et al., 2021). The FlocARAZI was designed to image flocculated suspended sediment in situ over the water column at depths up to 60 meters, identify sand within particle data, and estimate mass suspended sediment concentration (SSC) from image data. During deployment, a live video feed from the camera is transmitted via a Cat6 ethernet cable to a laptop at the surface where images are saved to the hard drive. A Sontek CastAway CTD is attached to the frame of the FlocARAZI to provide conductivity, temperature, and depth information for each image.

The FlocARAZI system itself consists of a camera, microscope lens, and LED light source situated within a waterproof housing. The camera system has a field of view of 3.7 x 2.8 mm and can resolve particles down to 6 microns. Suspended sediment is allowed to pass freely through a flow-through cell with a gap width of 1.17 mm. Images collected with the system are processed following the image processing routine developed by Keyvani and Strom (2013), with modifications outlined in Osborn et al. (2021). The relevant output from the image processing routine is the particle area in pixels^2, which is converted to an equivalent circular diameter. The particle diameter is converted from pixels to microns with 0.925 microns/pixel conversion factor. A processing routine utilizing a trained Support Vector Machine (SVM) classifier allows for identifying sand particles within the full particle data set, providing the means to isolate and analyze the flocculated and silt fraction of suspended sediment separate from the full imaged particle data set.

During deployment of the FlocARAZI, images are collected at a frequency of 2 Hz. With the CTD sampling initiated, the camera system was lowered in 3-meter increments from the free surface to the bed. At each increment over the water column, the FlocARAZI position was held steady for 1-2 minutes to collect approximately 90 images suitable for processing. While the FlocARAZI was deployed, velocity profiles were collected continuously with a Teledyne RiverPro Acoustic Doppler current profiler (ADCP). Velocity profiles were collected at an average sampling rate of 0.47 Hz with 0.69 to 0.85 m thick bins in the vertical.

Physical point samples of river water were collected at 5%, 25%, 50%, 75%, and 95% of the flow depth at each station using a USGS isokinetic P6 sampler. Collecting water samples consisted of holding the boat position steady, lowering the P6 to the predetermined depth, and opening the solenoid valve to fill a 1 L sample bottle. The solenoid is opened for a period of time ranging from 10 - 60 seconds depending on current speeds, allowing for the sample bottle to fill to approximately 75% capacity, ensuring the sample bottle is not overfilled during sampling. Water samples were filtered on-site with 1 μm glass fiber filters and the liquid volume of the sample was recorded. Once back in the lab, filtered water samples were allowed to dry in an oven at 80 degrees Celsius for 24 hours. The sample and filter were then weighed and the mass of the filter was subtracted to obtain the mass of the sample and hence the suspended mass concentration for each sample. Additional P6 samples were used to measure the disaggregated size distribution of the suspended material. These samples were dosed with sodium hexametaphosphate and sonicated prior to sizing with a LISST-Portable XR.

Bed material samples were collected at each station with a Shipek grab sampler. Samples were processed by first mixing the sediment until homogeneous. A subsample of the homogenized sample was then wet sieved with a No.230 (63 μm) mesh sieve to separate the fine and coarse sediment. The grain size distribution of the coarse fraction was obtained by sizing with a Retsch Technolog CAMSIZER.

2.5 Analysis calculations: settling velocity estimate through Rouse profile fit

The Rouse profile analysis includes fitting equation 5 to the measured concentration profiles using w_s as the fit parameter and then comparing these fit values of w_s to ones predicted from a settling velocity equation and the measured floc sizes. Data and parameters needed for the fit include the concentration profile data $C = C(z)$, the concentration at a reference height, C_b, a measure of u_* or for the station, and a measure of sediment stratification to account for the effects of turbulence damping, α.

For the analysis, data for $C = C(z)$ was obtained using data from the FlocARAZI following the methods presented in Osborn et al. (2021). For the winter surveys, SSC measurements were collected at all three stations included in the analysis (BCS, VMC, SWP1). For all three stations, the SSC measurements made with the P6 were used to inform the correction factor needed for FlocARAZI SSC measurements. The correction factor for each station was obtained by visually observing the best fit, by trial and error, between the SSC measured with the P6 and those estimated by the FlocARAZI. During the winter survey, a large amount of sand was present in suspension at the BCS. Therefore, the correction factor for the FlocARAZI SSC measurements was obtained by fitting the P6 SSC measurements to the total SSC estimated, including both mud and sand, with the FlocARAZI. Little sand was observed in suspension at the VMC or SWP1 stations during the winter survey, as such, both the SSC measured with the FlocARAZI and P6 water samples are assumed to contain little to no sand. For the summer survey, the reference depth and SSC were taken as the lowest depth where an SSC measurement was collected. The correction factor used for the SSC estimates from the summer survey were derived from an average of the correction factors used for the winter survey stations; concentration estimated with the camera using the winter calibration parameters fit within calculated concentrations from the Baton Rouge station (Table 1), resulting in slightly lower concentrations overall in summer relative to winter.

ADCP velocity data were used to obtain shear velocity estimates. The method for calculating u_* included taking the average flow velocity, u, at each depth interval against the natural log of the distance from the channel bed, z, fitting a line through the data, and multiplying the slope of the resulting line by $\kappa = 0.41$ (Eq. 2). When no bedforms are present, shear velocity calculated using this method was used directly in the Rouse profile calculations. To account for the impact of bedforms, the empirical relation developed by Wright and Parker (2004b) for large, low-sloping sand bed rivers was employed to estimate the non-dimensional skin friction shear stress, τ_{*s}, from which the skin friction velocity driving transport was obtained:

$$\tau_{*s} = 0.05 + 0.7(\tau_* \, Fr^{0.7})^{0.8} \tag{9}$$

In equation 9, τ_* is the total dimensionless bed shear stress, and Fr is the Froude number where $Fr = U/\sqrt{gH}$; where U is the depth-averaged velocity (obtained from ADCP measurements). By definition, the total dimensionless bed shear stress is:

$$\tau_* = \frac{u_*^2}{gR_s d} \tag{10}$$

with the dimensionless skin-friction shear stress, from which the needed skin-friction component of the shear velocity (u_{*s}) is obtained, being:

$$\tau_{*s} = \frac{u_{*s}^2}{gR_s d} \tag{11}$$

In all cases g is the acceleration due to gravity, d is the characteristic grain size, taken here as d_{50}, and R_s is the submerged specific gravity, given by $R_s = (\rho_s - \rho)/\rho$ where ρ_s is the density of the sediment, and ρ is the fluid density.

The effect of turbulence damping due to sediment stratification was accounted for by equation 8. To use equation 8, the volume concentration of sediment at 5% of the flow depth and the water surface slope are needed. C_{t5} was calculated assuming a sediment density of 2650 kg/m^3 and a water density of 1000 kg/m^3 in accordance with the method established in Wright and Parker (2004a). Estimates of the water surface slope were obtained from Nittrouer et al. (2011), where the authors present water surface slope measurements obtained upriver from Head of Passes under varying discharge ranges.

With the shear velocity and stratification parameter constrained, the only remaining variable within the Rouse number (Eq. 7) is the settling velocity, w_s. The settling velocity was obtained by performing a least squares regression analysis by fitting a Rouse profile to concentration data obtained from the FlocARAZI and physical water samples, allowing the settling velocity to vary.

2.6 Analysis calculations: settling velocity based on floc size

Expected values of w_s based on measured size were calculated using the settling velocity equation of Strom and Keyvani (2011). The equation is a modification of the solid particle settling velocity equation of Ferguson and Church (2004), and it is designed to work under both inertial and viscous settling conditions using the assumption that a floc of size d_f is a 3D fractal aggregate composed of primary particles of size d_p,

$$w_s = \frac{gR_s d_f^{n_f - 1}}{b_1 \nu d_p^{n_f - 3} + b_2 \sqrt{gR_s d_f^{n_f} d_p^{n_f - 3}}} \tag{12}$$

In equation 12, ν is the kinematic viscosity of the fluid. The coefficients b_1 and b_2 act as calibration coefficients that account for floc shape, permeability, and impacts from drag within the inertial range. Strom and Keyvani (2011) fit the model to a wide range of experimental and field floc data to obtain best fit values for b_1 and b_2 with the best correlation between the settling velocity curve and data when $n_f = 2.5$, $b_1 = 100$, and $b_2 = 0$.

3 Results

3.1 Overview

Depths at all sampling locations ranged from 17 to 25 m with depth-averaged velocity of ≈ 1 m/s near the BCS and $U \approx 0.75$ m/s at VMC (Table 2); overall, flow conditions at the VMC were less energetic than at the BCS. Salinity was near zero at all stations, uniform over the depth, and very close in absolute reported PSU values to the accuracy of the instrument (±0.1 PSU). In general, specific conductance was slightly higher during summer than winter by 100 to 200 µmS/cm. The bed material at the BCS was composed of sand (d_{50} = 0.22 mm) during both the summer and winter surveys, and significant dunes were observed through the ship's onboard sonar. The bed material at the VCM station during summer was also composed of sand (d_{50} = 0.20 mm) and dunes of significant size were again evident in the ship's sonar. However, during the winter survey, the bed at the VMC station was unconsolidated mud (90.3% of the material was < 63 μm) with no evident bedforms. Similar bed composition and morphology were observed downstream at SWP1.

Station	U [m/s]	H [m]	u_* [m/s]	u_{*s} [m/s]	S_0	Bed	C_b [mg/L]	SpC [µS/cm]	S [PSU]
BCS Summer	1.05	23.0	0.094	0.037	1.5E-05	Sand	136	440	0.20
VMC Summer	0.76	18.0	0.063	0.026	6.0E-06	Sand	122	395	0.18
BCS Winter	0.89	20.5	0.098	0.037	2.0E-05	Sand	160	215	0.16
VMC Winter	0.79	18.5	0.05	–	6.0E-06	Mud	268	271	0.19
SWP1 Winter	0.62	17.0	0.04	–	6.0E-06	Mud	484	275	0.19

Table 2. Measured hydraulic and water quality parameters. Water surface slope, S_0, was estimated from Nittrouer et al. (2011).

Suspended mud ($d < 63$ µm) from each station had a disaggregated d_{50} of approximately 6 to 15 μm. However, in situ images showed that at all sites, suspended mud was highly flocculated within the river (Figure 2) with a significant fraction of the material existing in aggregates that far exceeded 15 μm. The images also showed that some of the silt in suspension existed as individual free solid particles, but that much of the silt, even up to 63 µm in size, was bound within large floc aggregates similar to Tran and Strom (2017). This was true regardless of season, river station, or depth. This broadly confirms that similar to other rivers (Droppo & Ongley, 1994) and flume studies (Schieber et al., 2007), salty marine water is not necessary for mud in the Mississippi River to exist in flocculated form. Studies such as Galler and Allison (2008) and Lamb et al. (2020) have pointed to the possible role of flocculation on the transport dynamics of the Mississippi River, but images from the FlocARAZI confirm for the first time that suspended Mississippi River mud is indeed flocculated during both summer and winter.

3.2 The vertical and lateral distributions of floc d_{50}

The d_{50} by volume of the flocculated sediment is plotted over the depth for the BCS and VMC stations during summer and winter in figure 3. During the summer survey, floc size data were collected at two lateral locations at the BCS station and three lateral locations at the VMC station; indicated in Figure 3 a and b as being either the left bank, thalweg, or right bank. Floc size data were collected only at the thalweg location during the winter survey after observing little variation in size at different lateral stations across the section in the summer data.

No clear and consistent pattern in the d_{50} of the flocculated sediment with depth could be found in the data. Measured d_{50} values did fluctuate, and some trends with depth are present for some of the profiles, but no overall clear trend regarding the vertical distribution of d_{50} can be made that applies to all stations and seasons.

The floc d_{50} at the BCS during the summer ranged from approximately 75 to 100 μm near the bed, and 75 to 175 μm further up in the water column (Fig. 3a). A slight

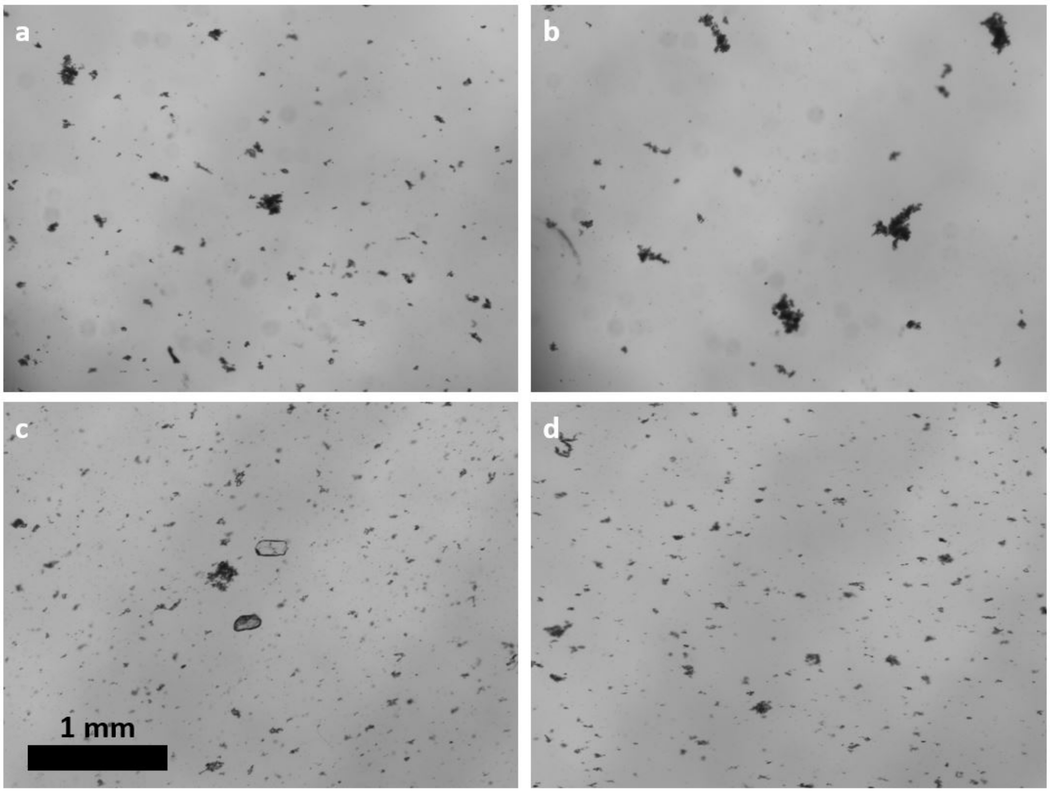

Figure 2. Example images collected during the summer at the (a) BCS and (b) VMC, and during the winter at the (c) BCS and (d) VMC.

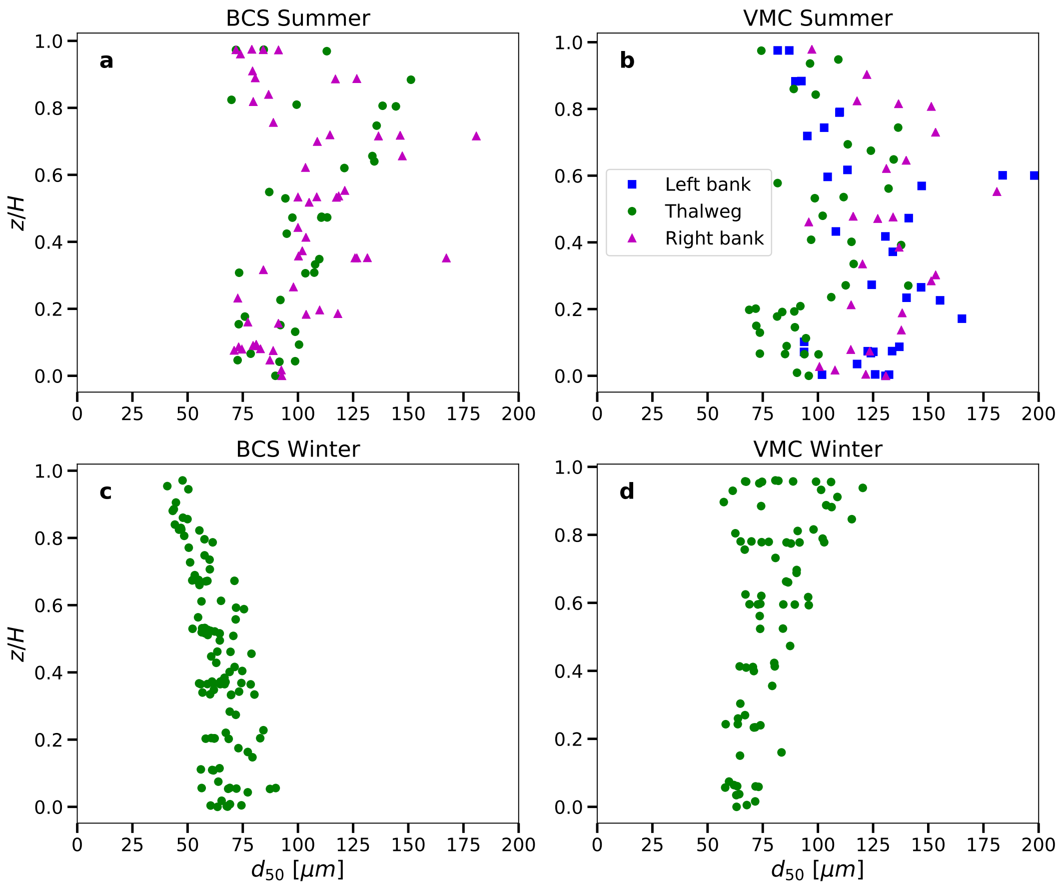

Figure 3. d_{50} floc size information collected at the BCS and VMC locations during the summer and winter surveys. Floc size data were collected at multiple lateral locations during the summer survey, as indicated in (a) and (b). Floc size data were collected only in the thalweg during the winter survey (c and d). Though it appears that floc size increases with depth at the winter BCS station (c), this is a result of a large fraction of the observed particles consisting of silt and fine sand that could not be removed in the image processing. As such, the size information presented in (c) represents the d_{50} of flocs, coarse silts, and fine sands.

increase in floc size from the bed to around 75% of the flow depth is present, with a slight decrease in floc size near the water surface for the right bank station. Average floc d_{50} at the VMC location during the summer survey range from around 75 μm to around 135 μm near the bed (Fig.3b). Floc sizes from the surface to around 25% of the flow depth are relatively uniform, ranging from around 100 to 150 μm. The largest flocs were observed at the left and right bank stations, where the largest d_{50} values were between 175 and 200 μm. d_{50} values at the VMC station during the winter ranged from around 60 μm near the bed to between 50 to 125 μm near the surface (Fig. 3d). Floc sizes near the bed vary only slightly, between 55 to 75 μm, compared to further up in the water column where both average d_{50} floc sizes increase and the range of sizes increases.

Though flocs were observed in suspension at the BCS during the winter survey, the data presented in Figure 3c represents the d_{50} sizes of flocs, silts, and fine sands. This is a result of the turbid conditions and images collected with the FlocARAZI containing a large amount of silt and sand. The algorithm used for identifying sand from image data was unable to correctly identify sand when flocs or silts overlapped with sand within the images. Medium to large sand was manually removed from the data, but a large number of very fine sand grains within the data made it unfeasible to manually remove them from the data set. Therefore, the data presented in Figure 3c should not be taken to represent only floc sizes at the winter BCS location.

3.3 Floc populations and their variation with depth

A range of floc sizes was observed at all locations and depths. The previous section showed how the d_{50} of the size population varied over the depth at different stations and seasons. In this section, we show the distributions. The distributions are visualized as kernel density estimates (KDE) (Figs. 4) and volume percent of flocs in a specified size range (Fig. 5) at 7.5%, 25%, 50%, 75%, and 92.5% of the flow depth.

Two general statements regarding the distribution of flocs sizes can be made. The first is that all distributions contained one dominant peak in size (Fig. 4). The second is that clustering of flocs within particular larger size classes was found to be present for flocs greater than approximately 100 μm. This clustering can be seen in the right-side tails of the KDE plots as a change in slope (Fig. 4). No clear number of, or locations for, the inflection points applicable to all distributions is evident.

In all cases flocs in the 50 to 100 μm size range make up the bulk of the flocculated material by volume, i.e., $\approx$ 40% (Fig. 5) with the 100 to 150 μm range making up $\approx$ 20 to 30%. This means that about 60 to 70% of the flocculated mud, by volume, is between 50 and 150 μm in size. The largest flocs, > 150 μm, compose 20 to 30% on average with the smallest flocs, < 50 μm, makeup 10 to 20% on average (though this percentage for the smallest size class was higher for the VMC during winter).

Changes in the distribution of these size fractions over the depth were relatively minor except when closest to the bed ($z/H = 0.075$) during summer. For both BCS and VMC, the binned data shows a general decrease in the fraction of large flocs closest to the bed (Fig 5a and b). This decrease in the fraction of flocs in the larger size classes (> 150 μm) was then accompanied by an increase in flocs within the smaller size classes. Another trend evident is that the percentage by volume of largest flocs tended to increase slightly moving from the bed towards the free surface for both the BCS and VMS during summer and the VMC during winter. The one exception to this was the topmost point at BCS during summer (Fig 5).

The BCS winter KDE and volume percent of binned particles plots show a coarsening of suspended sediment from the surface to the bed (Figs. 4c and 5c). Again, this is a result of the data for this particular station representing flocs, silts, and very fine sands as previously noted.

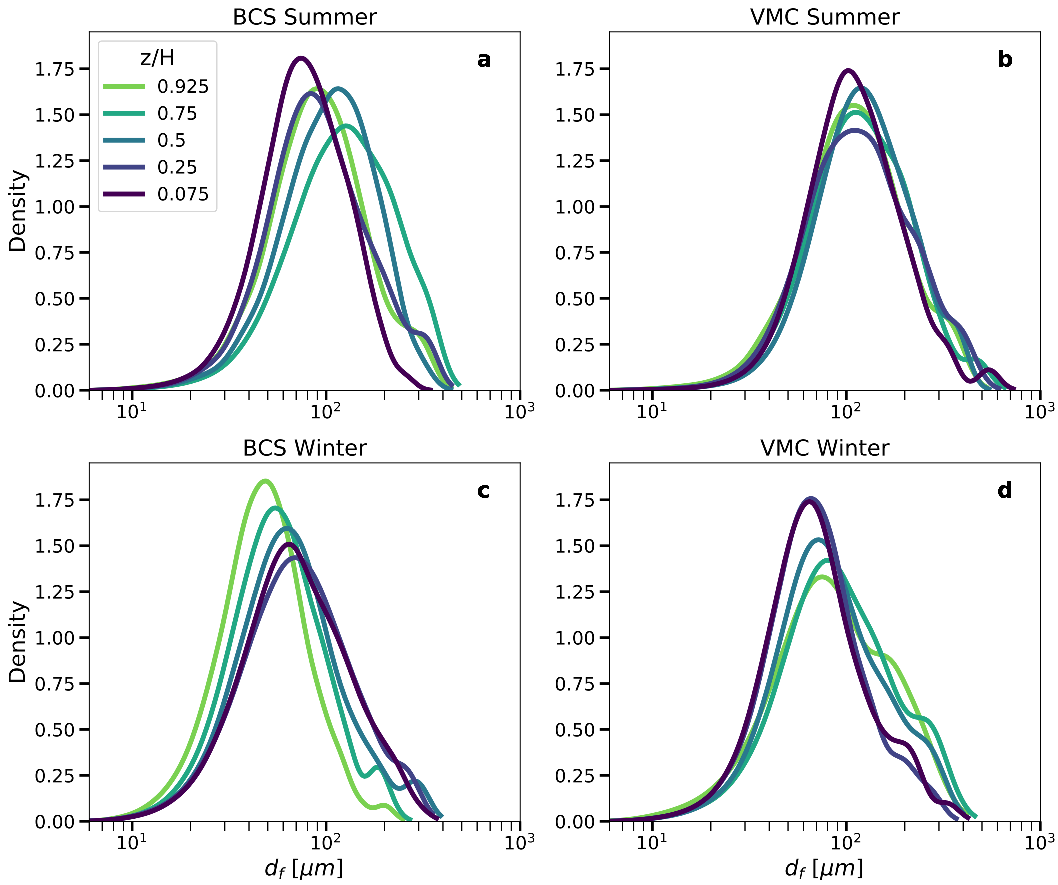

Figure 4. Kernel density estimates (KDE) of the probability density function for floc size population data collected over specified ranges within the flow depth. Here z is taken as the vertical distance from the bed and H is the flow depth.

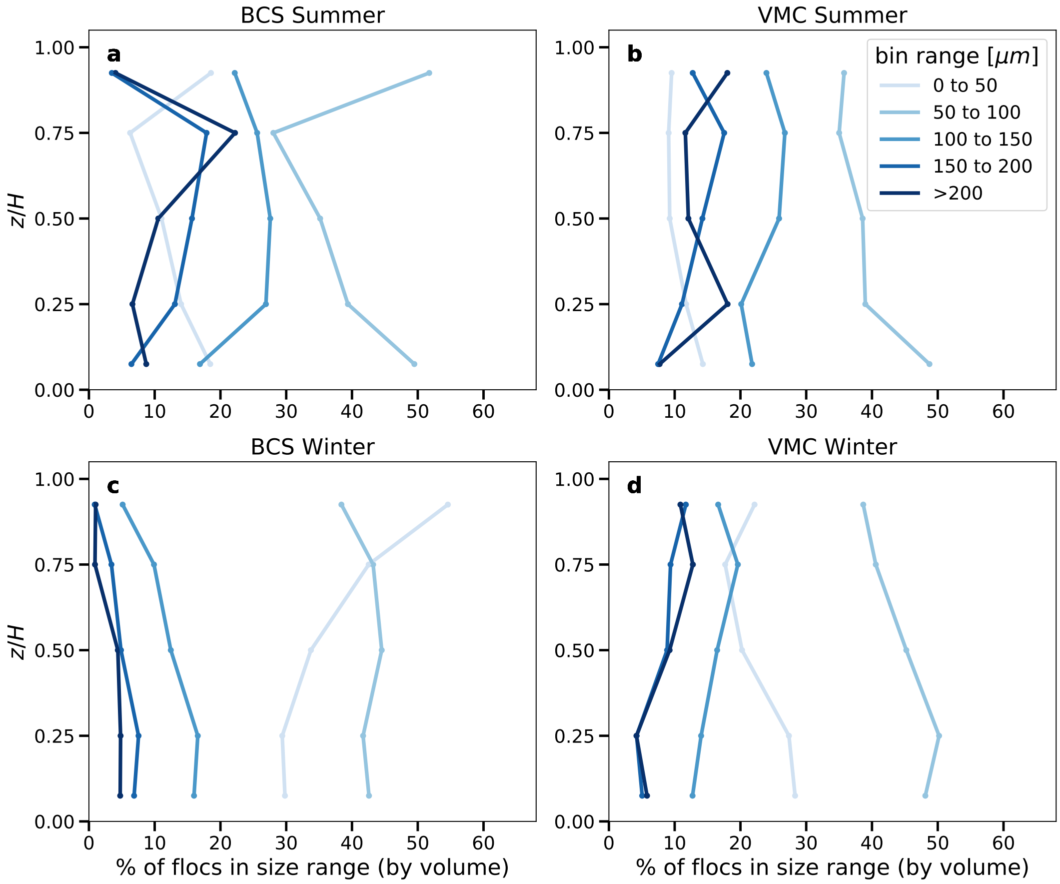

Figure 5. Floc size binned by volume into different size ranges at 7.5%, 25%, 50%, 75%, and 92.5% of the flow depth. Here z is taken as the vertical distance from the bed and H is the flow depth.

3.4 Depth-averaged trends in size by station and season

Depth-average values for the size statistics d_{16}, d_{50}, and d_{84} were calculated to allow for comparison of the average floc properties at different river stations in the same season and different seasons at the same station. During the same season, there was a small but noticeable change in the average size of the flocs moving down the river from the BCS to the VMC. On average, flocs at the VMC were larger than those at the BCS regardless of the season. For a given season, d_{50} increased by 10 to 15 μm going from the BCS to the VMC stations with d_{84} increasing by 30 to 40 μm (Table 3). This spatial change is possibly related to the overall decrease in river velocity and stress going from the BCS down to VMC (Table 2).

A difference in the depth-averaged size of the flocs between seasons was observed at each station, and the magnitude of the seasonal difference was greater than that between stations during the same season. At both stations, the floc d_{50} was ≈ 40 μm larger during the summer survey, with the d_{84} being ≈ 60 μm larger during the summer (Table 3). The 40 μm difference at the BCS was true even though the winter size estimates were biased larger due to the presence of solid particles that could not be removed during image processing as previously discussed. The difference in floc sizes is also evident in the sample images from each station and survey (Fig. 2).

Station	d_{16} [μm]	d_{50} [μm]	d_{84} [μm]
BCS Summer	57	102	185
VMC Summer	66	116	213
BCS Winter*	35	63	119
VMC Winter	44	79	160

Table 3. Average floc sizes for main channel stations. *The BCS winter station includes both flocs and fine sand.

3.5 Floc settling velocity and mud concentration profiles

A Rouse profile was fit to the mud fraction of suspended sediment using SSC profiles collected at the BCS and VMC during both the summer and winter surveys. In addition, SWP1 from the winter survey is included in the analysis. Measured and calculated input parameters used for the analysis are presented in Table 2. In Table 2, values for the skin friction component of shear velocity were excluded for VMC and SWP1 during the winter survey since the bed consisted mainly of mud, and no bedforms were observed during the survey. The fit results are shown in Figure 6.

During the summer survey, settling velocities from the fit were 0.41 mm/s at the BCS and 0.52 mm/s at the VMC location (Fig. 6a and b). This increase is consistent with the increase in floc size moving from the BCS to the VMC stations. During winter effective settling velocity estimates from the fit were smaller for the BCS station relative to summer ($w_s = 0.07$ mm/s) due to the near well-mixed conditions that existed for $C = C(z)$ (Fig. 6c). However, larger vertical concentration gradients of mud were observed downriver at VMC and SWP (Fig. 6d and e). For these two locations during winter, the effective settling velocities obtained from the fit were 2.3 and 2.9 mm/s. Possible explanations for these high settling velocity estimates, relative to the other stations, are considered in the Discussion.

Settling velocity was also calculated using the measured floc sizes and equation 12. The following input values were used to make the calculations: ν and ρ were adjusted

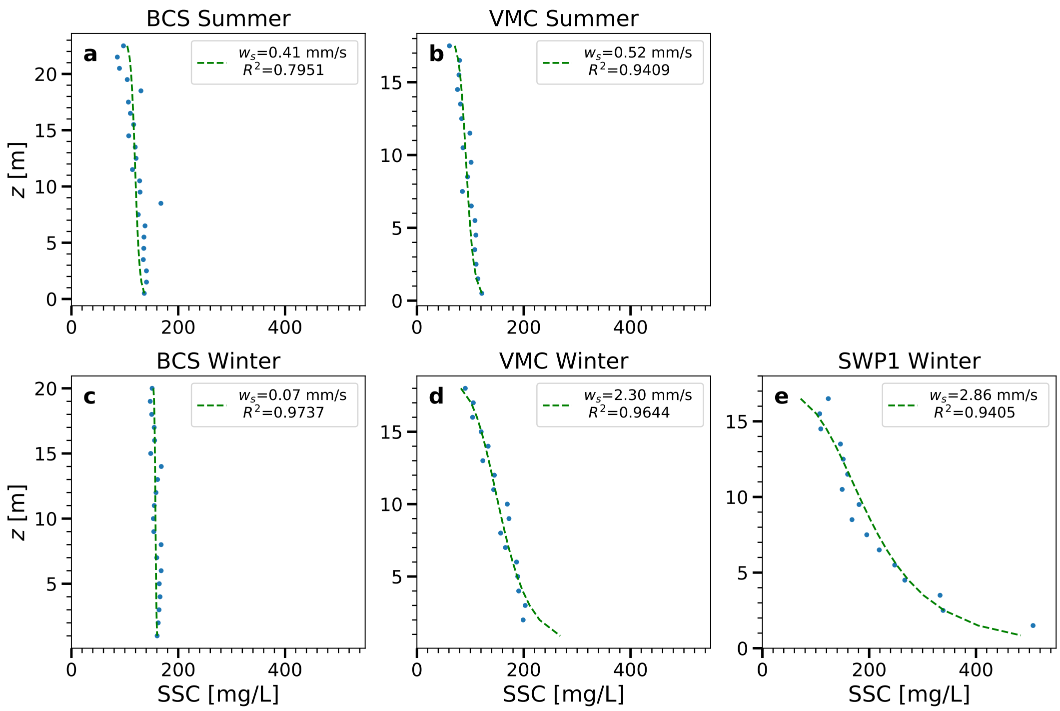

Figure 6. Mud fraction of SSC and fit Rouse profiles used to obtain an estimated bulk settling velocity.

for water temperature during the summer and winter; the primary particle size, d_p was taken as 6 μm based on measurements of disaggregated samples; the density of the primary particles was taken to be $\rho_s = 2650$ kg/m^3. Two sets of values for the coefficients b_1 and b_2 and the fractal dimension, n_f, were used. As a first pass, we used the viscous settling values of $b_1 = 100$, $b_2 = 0$, and $n_f = 2.5$ as suggested by Strom and Keyvani (2011) based on their fitting of historic floc settling data to estimate w_s based on the measured floc sizes. For the second set of coefficients, we used the standard values of $b_1 = 20$ and $b_2 = 0.91$ as suggested by Ferguson and Church (2004) based on the settling of solid sand using nominal, rather than sieved, particle size. We then varied the fractal dimension until the calculated value based on floc size matched the value obtained from the Rouse profile fit. In all cases, a bulk, volume-weighted settling velocity for the n number of flocs, with a volume, $\forall_{f,i}$, was calculated as: $w_s = \sum_{i=1}^{n} w_{s,i} \forall_{f,i} / \sum_{i=1}^{n} \forall_{f,i}$. The bulk settling velocity was calculated for the full set of flocs observed at a particular station.

For the BCS and VMC summer stations, the viscous model coefficients and fractal dimension of $n_f = 2.5$ yielded average settling velocity values that well matched those from the Rouse profile analysis (Table 4). Exact matches were found for these two summertime locations with the viscous coefficients by letting $n_f = 2.4$. During the winter, the viscous model performed reasonably well in terms of estimating the average settling velocity obtained from the Rouse profile fit at the BCS station. However, the calculated values were an order of magnitude smaller than the Rouse estimates during winter at the VMC and SWP1 stations.

No match could be found between the profile estimates and size-based estimates of settling velocity during winter at VMC and SWP1 when using the viscous coefficients of $b_1 = 100$ and $b_2 = 0$ for any fractal dimension $\leq$ 3. To obtain a match for these two stations, we used the Ferguson and Church (2004) recommended solid sand coeffi-

Station	w_s [mm/s] Rouse fit	w_s [mm/s] Size-based calculations*	n_f Fit based on sand coef.†
BCS Summer	0.4	0.5	1.90
VMC Summer	0.5	0.6	1.95
BCS Winter	0.1	0.2	1.50
VMC Winter	2.3	0.3	2.70
SWP1 Winter	2.9	0.3	2.70

Table 4. Settling velocities estimated from the Rouse profile analysis compared to calculations based on measured floc sizes and the settling velocity equation (eq. 12). *Calculations performed using the viscous floc settling coefficients of $b_1 = 100$, $b_2 = 0$, and $n_f = 2.5$. † Fractal dimensions, n_f, needed to make the calculated settling velocity, based on the nominal sand diameter coefficients of $b_1 = 20$ and $b_2 = 0.91$, match the settling velocity obtained from the Rouse profile fit.

cients of $b_1 = 20$ and $b_2 = 0.91$ and varied n_f until the w_s matched that from the Rouse fit. The same calculation was also performed on all other stations, and the output of the calculation is given in the last column of Table 4. In summary, the fractal dimension needed for summer was $n_f \approx 1.9$ and for winter $n_f \approx 2.7$.

4 Discussion

4.1 Spatial distributions of floc sizes and the role of turbulence and concentration in setting floc size

Our study confirms that flocs are present within the freshwater reaches of the Mississippi River during both the summer and winter. To the best of our knowledge, this study presents the first direct in-situ observations of flocs within the Mississippi River. Galler and Allison (2008) investigated the possibility of mud flocculation within the lower Mississippi River by collecting water samples with Niskin bottles to perform settling column tests on board their research vessel during a survey in June 2003. The observed settling rates led Galler and Allison (2008) to estimate that a third of the sediment mass within the settling column consisted of flocs smaller than 110 μm, and another third of the mass consisted of flocs larger than 567 μm. This range of floc sizes is in the range of floc sizes observed directly in this study during the summer survey. Similar mean floc sizes, in the range of 43 to 181 μm were observed with a LISST-100x at 23 stations along 1532 km of the Yangtze River by L. Guo and He (2011).

We were unable to detect any consistent and persistent patterns in the distribution of floc sizes either laterally across the river or vertically over the depth. For this reason, as a first approximation, we suggest that floc sizes at a given river station can be assumed to be uniformly distributed over the cross-section. During some of the samplings, we did observe a clear trend of higher numbers of larger flocs near the free surface and higher numbers of smaller flocs near the boundary; a trend that has also been observed in some estuaries using a LISST-100x (e.g., Huang et al., 2022); though the trend is not consistent in all estuaries and often depends on the position in the tide cycle (e.g., Uncles et al., 2010; C. Guo et al., 2017). This type of distribution in size over the depth is perhaps explained by the increase in turbulent production and dissipation rate of turbulent kinetic energy near the boundary and the known inverse relationship between floc size and dissipation rate (Tambo & Hozumi, 1979; van Leussen, 1994; Verney et al., 2009; Kuprenas et al., 2018). Nevertheless, the pattern of larger flocs near the free surface and smaller flocs near the bed was not always observed. In addition, larger flocs were not correlated with the higher concentrations of mud found near the boundary. At all stations, mud concentration increased with depth regardless of river station or season (though the strength of the stratification with depth and station did vary). However, such increases in concentration with depth were not correlated with an increase in floc size. We, therefore, expect that floc sizes can respond to the overall average concentration in the river, but are less influenced by local depth-dependent variations in concentration; at least over the range of conditions we observed.

Floc sizes did respond as expected to changes in overall average shear. The Mississippi River at the BCS is narrower and more energetic than it is farther down the river at the VMC station. Velocities and shear velocity measurements are reflective of this with higher values at BCS relative to the VMC and water column and image samples both reveal more sand in suspension at the BCS relative to the VMC station. Overall average concentration between the two sites was nearly equal with concentrations at the BCS being slightly larger. Floc sizes however were larger at the VMC during both seasons, indicating the floc size is dependent on the shear rate in the river but not on small changes in concentration.

4.2 Seasonal effects on floc size

The differences in floc sizes over the depth, or from station to station, were all smaller than the differences in floc sizes observed from the summer to winter surveys at each individual station. Both summer and winter surveys took place during relatively high flow conditions at similar discharges, though the summer survey was made on the falling limb of a flow event and the winter survey was made on the rising limb. Average velocities and shear stresses were similar at each station from season to season. And turbidity measurements and calculated average suspended sediment values were also similar between the two surveys; though C_{avg} was slightly higher on average during the winter (Table 1).

While the flow rate, shear stress, and suspended sediment concentration were similar from survey to survey, differences in floc sizes between summer and winter were observed. Flocs were substantially larger during summer than they were during winter. The d_{50} of the floc size distribution was approximately 40 µm larger in summer than in winter. The size difference in flocs between summer and winter could not have been due to differences in suspended sediment concentration since concentration was slightly larger during the winter. We also don't expect the size difference to be an outcome of changes in viscosity and hence the Kolmogorov micro length scale. The lower water temperature in winter should have led to larger micro length scales given the same overall average shear velocity and hence larger flocs in winter if the size difference were driven by turbulence conditions in the water column. Therefore we do not expect that the differences in floc size were driven by physical changes in turbulence or suspended sediment concentration. Instead, we expect that the difference in size was driven by differences in the chemistry (ion composition and concentration) or biology (organic material type and quantity) of the suspensions.

Water quality measurements made by the USGS at the Belle Chasse gage station 07374525, located between the BCS and VMC, over dates closest to our survey are listed in Table 5. Specific conductance and ion composition and concentration are fairly consistent between the summer and winter, though specific conductance and the calcium and magnesium levels are all slightly higher during summer relative to winter (Tables 2 and 5). Abolfazli and Strom (2022) have shown that the presence of calcium chloride and magnesium chloride both can have a stronger influence on the flocculation potential of a suspension of natural mud than sodium chloride, and data from the Belle Chasse station do indicate that these ions were present at a slightly higher concentration dur-

Parameter	Summer	Winter
Date	2020-06-23	2021-01-12
T [deg C]	27.4	6.9
SC [µS/cm]	362	348
pH	7.4	7.9
DO [mg/L]	5.9	12.1
N [mg/L]	2.3	1.7
P [mg/L]	0.18	0.32
DOC [mg/L]	3.4	2.95
Ca [mg/L]	40.6	30.9
Mg [mg/L]	14	10.3
Na [mg/L]	14	21.4
K [mg/L]	3.19	2.76
Cl [mg/L]	15.8	28.6
Fe [µg/L]	15.5	460

Table 5. Water quality measurements at USGS gage station 07374525 Mississippi River at Belle Chasse, LA over dates closest to the survey study date. The Belle Chasse station is located between the Bonnet Carré Spillway and Venice Main Channel sampling locations.

ing summer. However, the overall specific conductance values, while larger than those of headwater creeks (0 to 100 µS/cm), are nowhere near levels significant enough to produce 1 PSU, and it is unclear if the variation between summer and winter in terms of specific conductance (Table 2) is sufficient to account for the 40 µm change in the floc d_{50}. We suspect that it is not and that the difference in floc size between summer and winter is likely not driven by differences in ion concentration or type. pH is also known to influence flocculation rates and equilibrium size (Mietta et al., 2009), but the pH of the river varied little between our summer and winter surveys (Table 5).

The largest detectable difference from summer to winter in both our measurements and the water quality measures at the Belle Chasse station was that of water temperature (27 °C during summer and 6 °C during winter). Some water-treatment-focused studies have shown that temperature can change the optimum pH for flocculation at particular doses of some coagulants (Camp et al., 1940; Mohtadi & Rao, 1973), and in some cases, floc size (Fitzpatrick et al., 2004). However, as of yet, there is little evidence that temperature alone can change the flocculation behavior of natural mud (Mohtadi & Rao, 1973). Therefore we do not expect that temperature itself was directly responsible for the difference in size observed between the seasons.

Taking all of the above into consideration, we suspect that a temperature-driven difference, or temperature co-varying difference, in a particular type of organic content is likely the leading cause of the observed difference in floc sizes between summer and winter. Organic content comes in many different forms. The most common measurement of organic content is that of Dissolved Organic Carbon (DOC). Yet, DOC does not vary significantly with season or discharge in the Mississippi River (e.g. Table 5), though it can be slightly higher during warmer temperatures and higher discharges (Cai et al., 2015). Furthermore, DOC concentration increases during high flows might primarily be sourced from organic constituents associated with terrestrial runoff that may or may not contribute to floc formation (Lee et al., 2019). What is known to enhance flocculation is EPS. EPS is known to be positively associated with Chlorophyll-a (Uncles et al., 2010) through algal production (Verney et al., 2009; Lee et al., 2019), and particle-attached bacterial communities. In the Mississippi and elsewhere, increases in Chlorophyll-a are associated with warmer water temperatures and low-flow periods where mixing and sediment con-

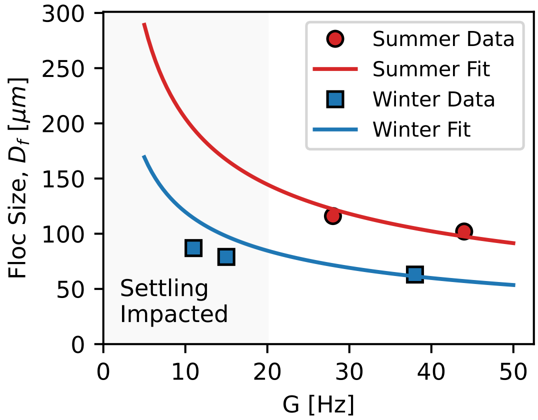

Figure 7. A model for equilibrium floc size as a function of concentration and shear rate, $d_{fe} = d_{fe}(C, G)$, fit to the summer and winter depth-averaged floc sizes at different river stations.

centration are lower (Duan & Bianchi, 2006; Turner et al., 2022; Lee et al., 2019). Discharge conditions during the summer survey were not particularly low (Table 1) with respect typical discharges associated with high Chlorophyll-a values (< 15,000 m^3/s) (Turner et al., 2022).

Bacterial production, and specifically particle-associated bacterial production, is known to be strongly dependent on temperature in the Mississippi River regardless of flow discharge (Ochs et al., 2010; Payne et al., 2020). Therefore, we suspect that the increase in observed floc sizes in the summer was primarily due to the increased activity of particle-attached bacterial secreting EPS and enhancing the capture potential and strength of the mud aggregates. Similar correlations between water temperature and floc size and strength have been made by Droppo et al. (1998) and Egan et al. (2022), both of whom suggest that increasing temperature leads to an increase in the productivity of the particle-attached bacteria and associated enhancement of EPS. Therefore, while tightly controlled data linking floc size to increased bacterial production brought on by temperature changes is not available in our study or the studies of Droppo et al. (1998) and Egan et al. (2022), all three point to the utility of temperature as a proxy for EPS production and hence floc aggregation efficiency and strength. For example, calibration of the equilibrium floc size model (see appendix for details), which yields $d_{fe} = d_{fe}(C, G)$, of Winterwerp (1998) can be made for summer and winter along the Mississippi at the different stations by increasing the ratio of the aggregation to breakup efficiency terms, k'_A/k'_B, by a factor of 5 (Figure 7). It is conceivable then, that given enough data, one could develop a relationship for $k'_A/k'_B = k'_A/k'_B(T)$.

4.3 Can floc size explain vertical gradients in mud concentration?

Flocculation has the potential to increase the settling velocity of mud relative to that predicted by the disaggregated particle sizes. For example, the calculated settling velocities for the summer survey at the BCS and VMC range from 0.41 to 0.53 mm/s. These settling velocities correspond to an equivalent silt grain with a diameter between 25 to 30 μm. However, considering that the characteristic primary particle size that makes up the flocs is likely between 5 and 10 μm, the calculated floc settling velocities are approximately an order of magnitude higher than the settling velocity of the characteristic primary particles.

If mud within a river is unflocculated, the unaggregated particles would be expected to be distributed uniformly over the water column as a result of their small settling velocities. However, it is possible that the presence of flocs, and hence increased settling velocity of the mud, could result in vertical concentration gradients of mud in rivers. Recently Lamb et al. (2020) analyzed disaggregated mud size and concentration profile data obtained from a range of lab and field measurements. They hypothesized that if flocculation of mud was present, this could be observed through vertical variations in mud concentration of individual grain-size classes. That is, vertical variations in concentration would be present for size classes that would be expected to be distributed uniformly over the water column if no flocculation was present. They tested this hypothesis by analyzing individual grain-size classes from the mud size and concentration data, from the multiple data sources, in a Rouse profile analysis to obtain effective settling velocities for each grain-size class. Their results indicated that mud effective-settling velocities range from 0.17 to 0.70 mm/s, with a geometric mean of 0.34 mm/s. This range of settling rates is in agreement with the 0.2 to 0.6 mm/s settling velocity of mud calculated in this study from direct observations of mud floc sizes in the lowermost Mississippi River during the summer and winter.

The settling velocities calculated from observed sizes well matched those calculated from the Rouse profile analysis for all summer survey locations and the BCS during winter. Therefore we conclude that flocculated mud was the primary driver of the observed concentration gradients during summer. However, estimated settling velocity from the Rouse profile during winter at VMC and SWP1 produced settling velocities that far exceeded those of summer and produced a significant mismatch between the Rouse profile estimated settling velocity and bulk settling velocity calculated from the floc size distributions (when using w_s model coefficients of $b_1 = 100$, $b_2 = 0$, and $n_f = 2.5$). Possible explanations for the mismatch at least include:(1) the assumption that form drag is insignificant is incorrect and should be accounted for in the shear velocity; (2) the possibility that a significantly more free or floc-bound silt was present in winter relative to summer; and (3) the mud bed observed at VMC and SWP1 during the winter was net erosional as river discharge increased over the course of the survey, violating the Rouse profile assumption that erosion of the bed is in equilibrium with deposition and thereby resulting in higher near-bed concentrations than would be expected under equilibrium conditions.

The assumption that the form drag component of shear velocity was negligible during the winter survey at VMC and SWP1 was made as a result of not observing large-scale bedform contours from single-beam sonar images observed while onboard the research vessel. If the skin friction component of shear velocity at VMC and SWP1 during the winter was calculated with equation 9, the values associated with the stations would decrease to 0.023 m/s and 0.018 m/s. Applying this decrease in shear velocity to the Rouse profile analysis reduces the estimated settling velocities to 1.07 and 1.32 mm/s for VMC and SWP1 during the winter survey — a nearly 54% decrease in estimated settling velocity at both stations. However, even if form stress was removed via equation 9, w_s from the Rouse profile fit would still be significantly larger than those calculated from imaged particle sizes with the $b_1 = 100$ and $b_2 = 0$ coefficients.

During the winter survey, water column samples were filtered directly for concentration without sizing of the particles. Therefore, it is possible that a larger amount of free or floc-bound silt was present in the samples, thereby resulting in overall larger suspension-average particle or floc density and higher settling velocities. From visual inspection of the images, we conclude that both free and floc-bound silt is present in suspension at all sampling locations during both summer and winter. Qualitatively, it did appear that there might have been a slightly larger volume of solid silt in the winter samples at VMC relative to that of summer. If true, the increase in silt content could be reflected in the increase in fit fractal dimensions at the site between summer and winter using the solid sand coefficients in the settling velocity equation and the Rouse profile measured settling velocity (Table 4). However, we were not able to rigorously quantify of the amount of free or floc-bound silt from the images. Therefore the visual-inspection observation remains highly speculative and in need of other forms of quantitative assessment.

An additional possible explanation for the higher estimated settling velocity obtained from the VMC and SWP1 data during the winter could be a result of net erosion of the mud bed. If this is the case, the assumption made in the Rouse profile derivation, that bed erosion and deposition are in equilibrium, would be violated and could lead to concentrations near the bed that are higher than what would be present during equilibrium conditions. It was hypothesized that the mud bed at VMC and SWP1 observed during the winter survey was deposited in the presence of a salt wedge that had migrated upriver past these stations as a result of low river discharge proceeding the survey. In the week leading up to the survey, river discharge had increased significantly and pushed the salt wedge out of the main channel. This increase in discharge could potentially produce a high enough bed shear stress to cause net erosion of the bed.

5 Conclusions

This study presents the first direct measurements of floc sizes within the lowermost freshwater reaches of the Mississippi River from the Bonnet Carré Spillway down through the head of Southwest Pass. Measurements were made at different longitudinal, lateral, and vertical positions within the river during summer 2020 and winter 2021 at a river discharge of ≈ 19,000 cms and average suspended sediment concentrations of ≈ 150 mg/l in both surveys. At all sampling locations, suspended mud flocs comprised of clay and silt were observed in both the winter and summer surveys. The exact proportion of the mud which exists in flocculated form is difficult to determine, but flocs were the dominant particulate form present in the images.

Depth-averaged floc sizes increased slightly moving longitudinally downriver as turbulence levels dropped, but floc sizes varied little over the flow depth or laterally across a cross-section. During the summer survey, mean floc sizes were observed to range from 75 to 200 μm. Whereas in the winter mean floc sizes ranged from 50 to 125 μm. Suspended sediment concentration profiles were used along with a Rouse profile fit to calculate an effective settling velocity of the suspension. Settling velocities calculated in this way were well explained by the measured floc sizes and floc model coefficients of $b_1 = 100$, $b_2 = 0$, and $n_f = 2.5$ during summer and winter at stations for which the bed remained sandy (or for a model with $b_1 = 20$, $b_2 = 0.91$, and $n_f = 1.90$). However, the measured floc sizes underestimated the settling velocities extracted from the concentration profiles during the winter survey at the stations for which there was a thick layer of unconsolidated mud with these same coefficients. To obtain particle-size derived settling velocities that matched those from the profile analysis, the settling velocity model coefficients had to be changed to $b_1 = 20$, $b_2 = 0.91$, and $n_f = 2.70$.

Overall, our study highlights that the majority of the mud (both silt and clay), in both summer and winter, in the lowermost freshwater reaches of the Mississippi River appears to be flocculated and that the floc size can be reasonably represented with a cross-sectionally averaged value that is dependent on turbulent shear and season. Floc size appears to well explain vertical variations in mud concentration in summer but failed to do so for the winter observations without changing of model coefficients. We suspect that this change is possibly due to a larger fraction of free or floc-bound silt in suspension and/or the presence of an actively eroding mud bed that results in disequilibrium conditions between erosion and deposition.

While these measurements point to the importance of flocculation in controlling mud settling rates in the Mississippi River, they also highlight the need for additional in-situ observations. More data is needed to fully understand the role of the hydrodynamic, suspended sediment quantity and composition, organic material, and ions in controlling floc size and settling velocities within the fluvial environment.

Acknowledgments

Funding for this work was provided by the National Science Foundation under EAR award 1801142, "Collaborative Research: Flocculation Dynamics in the Fluvial to Marine Transition." Additional financial support for R.O. was provided by the Charles E. Via, Jr. Endowment at Virginia Tech and the New Horizons Graduate Scholars Program. Upon publication, data associated with this study will be available at `https://github.com/FlocData/Data-Osborn-et-al-Mississippi`, or by contacting the corresponding author (strom@vt.edu).

References

Abolfazli, E., & Strom, K. (2022). Deicing road salts may contribute to impairment of streambeds through alterations to sedimentation processes. *ACS ES&T Water*.

Allison, M. A., Demas, C. R., Ebersole, B. A., Kleiss, B. A., Little, C. D., Meselhe, E. A., … Vosburg, B. M. (2012). A water and sediment budget for the lower Mississippi–Atchafalaya River in flood years 2008–2010: Implications for sediment discharge to the oceans and coastal restoration in Louisiana. *Journal of Hydrology*, *432–433*(0), 84 - 97.

Biedenharn, D. S., Copeland, R. R., Thorne, C. R., Soar, P. J., Hey, R. D., & Watson, C. C. (2000). *Effective discharge calculation: A practical guide* (ERDC/CHL No. TR-00-15). U.S. Army Engineer Research and Development Center, Coastal and Hydraulics Laboratory.

Bungartz, H., Krüger, A., & Engelhardt, C. (2006). Fluvial suspended sediment dynamics: Implications for particulate organic carbon transport modeling. *Water Resources Research*, *42*(10).

Cai, Y., Guo, L., Wang, X., & Aiken, G. (2015). Abundance, stable isotopic composition, and export fluxes of DOC, POC, and DIC from the Lower Mississippi River during 2006–2008. *Journal of Geophysical Research: Biogeosciences*, *120*(11), 2273–2288.

Camp, T. R., Root, D. A., & Bhoota, B. V. (1940). Effects of temperature on rate of floc formation. *Journal (American Water Works Association)*, *32*(11), 1913–1927.

Cartwright, G. M., Friedrichs, C. T., & Sanford, L. P. (2011). In situ characterization of estuarine suspended sediment in the presence of muddy flocs and pellets. In P. Wang, J. D. Rosati, & T. M. Roberts (Eds.), *The proceedings of the coastal sediments* (Vol. 1, p. 642-654).

Deng, Z., He, Q., Chassagne, C., & Wang, Z. B. (2021). Seasonal variation of floc population influenced by the presence of algae in the Changjiang (Yangtze River) Estuary. *Marine Geology*, *440*, 106600.

Droppo, I., & Ongley, E. (1994). Flocculation of suspended sediment in rivers of southeastern Canada. *Water Research*, *28*(8), 1799 - 1809.

Droppo, I. G., Jeffries, D., Jaskot, C., & Backus, S. (1998). The prevalence of freshwater flocculation in cold regions: A case study from the Mackenzie River Delta, Northwest Territories, Canada. *Arctic*, *51*(2), 155–164.

Droppo, I. G., Leppard, G. G., Flannigan, D. T., & Liss, S. N. (1997). The freshwater floc: A functional relationship of water and organic and inorganic floc constituents affecting suspended sediment properties. *Water, Air, & Soil Pollution*, *99*, 43-53.

Duan, S., & Bianchi, T. S. (2006). Seasonal changes in the abundance and composition of plant pigments in particulate organic carbon in the lower Mississippi

and Pearl Rivers. *Estuaries and Coasts*, *29*(3), 427–442.
Egan, G., Chang, G., Manning, A. J., Monismith, S., & Fringer, O. (2022). On the variability of floc characteristics in a shallow estuary. *Journal of Geophysical Research: Oceans*, *127*(6), e2021JC018343.
Eisma, D. (1986). Flocculation and de-flocculation of suspended matter in estuaries. *Netherlands Journal of Sea Research*, *20*(2-3), 183 - 199.
Fall, K. A., Friedrichs, C. T., Massey, G. M., Bowers, D. G., & Smith, S. J. (2021). The importance of organic content to fractal floc properties in estuarine surface waters: Insights from video, lisst, and pump sampling. *Journal of Geophysical Research: Oceans*, *126*(1), e2020JC016787.
Fennessy, M. J., Dyer, K. R., & Huntley, D. A. (1994). INSSEV: An instrument to measure the size and settling velocity of flocs in situ. *Marine Geology*, *117*, 107-117.
Ferguson, R., & Church, M. (2004). A simple universal equation for grain settling velocity. *Journal of Sedimentary Research*, *74*(6), 933-937.
Fettweis, M., & Baeye, M. (2015). Seasonal variation in concentration, size, and settling velocity of muddy marine flocs in the benthic boundary layer. *Journal of Geophysical Research: Oceans*, *120*(8), 5648-5667.
Fettweis, M., Schartau, M., Desmit, X., Lee, B. J., Terseleer, N., Van der Zande, D., ... Riethmüller, R. (2022). Organic matter composition of biomineral flocs and its influence on suspended particulate matter dynamics along a nearshore to offshore transect. *Journal of Geophysical Research: Biogeosciences*, *127*, e2021JG006332.
Fitzpatrick, C., Fradin, E., & Gregory, J. (2004). Temperature effects on flocculation, using different coagulants. *Water Science and Technology*, *50*(12), 171–175.
Fox, J., Ford, W., Strom, K., Villarini, G., & Meehan, M. (2013). Benthic control upon the morphology of transported fine sediments in a low-gradient stream. *Hydrological Processes*.
Galler, J. J., & Allison, M. A. (2008). Estuarine controls on fine-grained sediment storage in the Lower Mississippi and Atchafalaya Rivers. *Geological Society of America Bulletin*, *120*(3-4), 386-398.
Gibbs, R. J. (1985). Estuarine flocs: Their size, settling velocity and density. *Journal of Geophysical Research*, *90*(C2), 3249–3251.
Guo, C., He, Q., Guo, L., & Winterwerp, J. C. (2017). A study of in-situ sediment flocculation in the turbidity maxima of the Yangtze Estuary. *Estuarine, Coastal and Shelf Science*, *191*, 1 - 9.
Guo, L., & He, Q. (2011). Freshwater flocculation of suspended sediments in the Yangtze River, China. *Ocean Dynamics*, *61*, 371-386.
Horemans, D. M. L., Dijkstra, Y. M., Schuttelaars, H. M., Sabbe, K., Vyverman, W., Meire, P., & Cox, T. J. S. (2021). Seasonal variations in flocculation and erosion affecting the large-scale suspended sediment distribution in the Scheldt estuary: the importance of biotic effects. *Journal of Geophysical Research: Oceans*, *126*, e2020JC016805.
Huang, J., Wang, S., Li, X., Xie, R., Sun, J., Shi, B., ... Zheng, Z. (2022). Effects of shear stress and salinity stratification on floc size distribution during the dry season in the Modaomen Estuary of the Pearl River. *Frontiers in Marine Science*, *9*, 836927.
Izquierdo-Ayala, K., Garcia-Aragon, J. A., Castillo-Uzcanga, M. M., & Salinas-Tapia, H. (2021). Freshwater flocculation dependence on turbulence properties in the Usumacinta River. *Journal of Hydraulic Engineering*, *147*(12), 05021009.
Keyvani, A., & Strom, K. (2013). A fully-automated image processing technique to improve measurement of suspended particles and flocs by removing out-of-focus objects. *Computers & Geosciences*, *52*, 189-198.

Kim, J.-W., & Nestmann, F. (2009). Settling behavior of fine-grained materials in flocs. *Journal of Hydraulic Research*, *47*(4), 492-502.
Kranck, K. (1973). Flocculation of suspended sediment in the sea. *Nature*, *246*(5432), 348–350.
Kranck, K. (1980). Experiments on the significance of flocculation in the settling of fine-grained sediment in still water. *Canadian Journal of Earth Sciences*, *17*(11), 1517-1526.
Kranck, K., & Milligan, T. G. (1992). Characteristics of suspended particles at an 11-hour anchor station in San Francisco Bay, California. *Journal of Geophysical Research*, *97*(C7), 11373–11382.
Kuprenas, R., Tran, D., & Strom, K. (2018). A shear-limited flocculation model for dynamically predicting average floc size. *Journal of Geophysical Research: Oceans*, *123*, 6736-6752.
Lamb, M. P., de Leeuw, J., Fischer, W. W., Moodie, A. J., Venditti, J. G., Nittrouer, J. A., ... Parker, G. (2020). Mud in rivers transported as flocculated and suspended bed material. *Nature Geoscience*.
Le, H.-A., Gratiot, N., Santini, W., Ribolzi, O., Tran, D., Meriaux, X., ... Soares-Frazão, S. (2020). Suspended sediment properties in the Lower Mekong River, from fluvial to estuarine environments. *Estuarine, Coastal and Shelf Science*, *233*, 106522.
Lee, B. J., Hur, J., & Toorman, E. A. (2017). Seasonal variation in flocculation potential of river water: Roles of the organic matter pool. *Water*, *9*(5), w9050335.
Lee, B. J., Kim, J., Hur, J., Choi, I. H., Toorman, E. A., Fettweis, M., & Choi, J. W. (2019). Seasonal dynamics of organic matter composition and its effects on suspended sediment flocculation in river water. *Water Resources Research*, *55*(8), 6968-6985.
Lefebvre, J.-P., Ouillon, S., Vinh, V., Arfi, R., Panché, J.-Y., Mari, X., ... Torréton, J.-P. (2012). Seasonal variability of cohesive sediment aggregation in the Bach Dang–Cam Estuary, Haiphong (Vietnam). *Geo-Marine Letters*, *32*, 103-121.
Liss, S. N., Droppo, I. G., Flannigan, D. T., & Leppard, G. G. (1996). Floc architecture in wastewater and natural riverine systems. *Environmental Science & Technology*, *30*(2), 680-686.
Manning, A., & Dyer, K. (2002). A comparison of floc properties observed during neap and spring tidal conditions. In J. C. Winterwerp & C. Kranenburg (Eds.), *Fine sediment dynamics in the marine environment* (Vol. 5, p. 233 - 250). Elsevier.
Manning, A. J., & Dyer, K. R. (2002). The use of optics for the in situ determination of flocculated mud characteristics. *Journal of Optics A: Pure and Applied Optics*, *4*(4), S71.
Markussen, T. N., Elberling, B., Winter, C., & Andersen, T. J. (2016). Flocculated meltwater particles control Arctic land-sea fluxes of labile iron. *Scientific Reports*, *6*(1), 24033.
Marttila, H., & Kløve, B. (2015). Spatial and temporal variation in particle size and particulate organic matter content in suspended particulate matter from peatland-dominated catchments in Finland. *Hydrological Processes*, *29*(6), 1069-1079.
Mietta, F., Chassagne, C., Manning, A., & Winterwerp, J. (2009). Influence of shear rate, organic matter content, pH and salinity on mud flocculation. *Ocean Dynamics*, *59*(5), 751–763.
Mikkelsen, O. A., Hill, P. S., & Milligan, T. G. (2007). Seasonal and spatial variation of floc size, settling velocity, and density on the inner Adriatic Shelf (Italy). *Continental Shelf Research*, *27*, 417–430.
Mohtadi, M. F., & Rao, P. N. (1973). Effect of temperature on flocculation of aqueous dispersions. *Water Research*, *7*(5), 747–767.

Nghiem, J. A., Fischer, W. W., Li, G. K., & Lamb, M. P. (2022). A mechanistic model for mud flocculation in freshwater rivers. *Journal of Geophysical Research: Earth Surface*, *127*(5), e2021JF006392.

Nittrouer, J. A., Mohrig, D., & Allison, M. (2011). Punctuated sand transport in the lowermost Mississippi River. *Journal of Geophysical Research: Earth Surface*, *116*, F04025.

Ochs, C. A., Capello, H. E., & Pongruktham, O. (2010). Bacterial production in the Lower Mississippi River: importance of suspended sediment and phytoplankton biomass. *Hydrobiologia*, *637*(1), 19–31.

Osborn, R., Dillon, B., Tran, D., Abolfazli, E., Dunne, K. B. J., Nittrouer, J. A., & Strom, K. (2021). FlocARAZI: An in-situ, image-based profiling instrument for sizing solid and flocculated suspended sediment. *Journal of Geophysical Research: Earth Surface*, *126*, e2021JF006210.

Payne, J. T., Jackson, C. R., Millar, J. J., & Ochs, C. A. (2020). Timescales of variation in diversity and production of bacterioplankton assemblages in the Lower Mississippi River. *PLOS ONE*, *15*(4), e0230945–.

Phillips, J. M., & Walling, D. E. (1999). The particle size characteristics of fine-grained channel deposits in the River Exe Basin, Devon, UK. *Hydrological Processes*, *13*(1), 1–19.

Rouse, H. (1939). *An analysis of sediment transportation in the light of fluid turbulence* (Tech. Rep. No. SCS-TR 25). Washington D.C.: U.S. Department of Agriculture, Soil Conservation Service.

Schieber, J., Southard, J. B., & Thaisen, K. (2007). Accretion of mudstone beds from migrating floccule ripples. *Science*, *318*, 1760-1763.

Spencer, K. L., Wheatland, J. A. T., Bushby, A. J., Carr, S. J., Droppo, I. G., & Manning, A. J. (2021). A structure–function based approach to floc hierarchy and evidence for the non-fractal nature of natural sediment flocs. *Scientific Reports*, *11*(1), 14012.

Strom, K., & Keyvani, A. (2011). An explicit full-range settling velocity equation for mud flocs. *Journal of Sedimentary Research*, *81*(12), 921-934.

Tambo, N., & Hozumi, H. (1979). Physical characteristics of flocs-II: Strength of floc. *Water Research*, *13*(421-427).

Tan, X., Hu, L., Reed, A., Furukawa, Y., & Zhang, G. (2013). Flocculation and particle size analysis of expansive clay sediments affected by biological, chemical, and hydrodynamic factors. *Ocean Dynamics*, 1-15.

Thill, A., Moustier, S., Garnier, J.-M., Estournel, C., Naudin, J.-J., & Bottero, J.-Y. (2001). Evolution of particle size and concentration in the Rhône river mixing zone:: influence of salt flocculation. *Continental Shelf Research*, *21*(18), 2127–2140.

Tran, D., & Strom, K. (2017). Suspended clays and silts: Are they independent or dependent fractions when it comes to settling in a turbulent suspension? *Continental Shelf Research*, *138*, 81 - 94.

Turner, R. E., Milan, C. S., Swenson, E. M., & Lee, J. M. (2022). Peak chlorophyll a concentrations in the lower Mississippi River from 1997 to 2018. *Limnology and Oceanography*, *67*(3), 703–712.

Uncles, R. J., Bale, A. J., Stephens, J. A., Frickers, P. E., & Harris, C. (2010). Observations of floc sizes in a muddy estuary. *Estuarine, Coastal and Shelf Science*, *87*(2), 186–196.

Van der Lee, W. T. B. (2000). Temporal variation of floc size and settling velocity in the Dollard estuary. *Continental Shelf Research*, *20*, 1495–1511.

van Leussen, W. (1994). *Estuarine macroflocs and their role in fine-grained sediment transport* (Unpublished doctoral dissertation). University of Utrecht, The Netherlands.

Verney, R., Lafite, R., & Brun-Cottan, J.-C. (2009). Flocculation potential of estuarine particles: The importance of environmental factors and of the spatial

and seasonal variability of suspended particulate matter. *Estuaries and Coasts*, *32*(4), 678-693.
Winterwerp, J. C. (1998). A simple model for turbulence induced flocculation of cohesive sediment. *Journal of Hydraulic Research*, *36*(3), 309-326.
Woodward, J. C., & Walling, D. E. (2007). Composite suspended sediment particles in river systems: their incidence, dynamics and physical characteristics. *Hydrological Processes*, *21*(26), 3601–3614.
Wright, S., & Parker, G. (2004a). Density stratification effects in sand-bed rivers. *Journal of Hydraulic Engineering*, *130*(8), 783-795.
Wright, S., & Parker, G. (2004b). Flow resistance and suspended load in sand-bed rivers: Simplified stratification model. *Journal of Hydraulic Engineering*, *130*(8), 796-805.

Appendix A Equilibrium Floc Size Model Fit

The equilibrium floc size model of Winterwerp (1998) for $d_{fe} = d_{fe}(C, G)$ takes the following basic form:

$$d_{50} = d_p + \frac{k_A C}{k_B \sqrt{G}} \tag{A1}$$

where d_p is the disaggregated primary or constituent particle size, C is the mass concentration of sediment, and k_A and k_B are the aggregation and breakup coefficients defined as:

$$k_A = \frac{k'_A}{n_f} \frac{d_p^{n_f - 3}}{\rho_s} \tag{A2}$$

and,

$$k_B = \frac{k'_B}{n_f} d_p^{-p} \left(\frac{\mu}{F_y}\right)^q \tag{A3}$$

In Eq. A2 and A3, n_f is the fractal dimension of the flocs, ρ_s density of the dry unflocculated sediment, μ is the dynamic viscosity of the water, F_y is the yield strength of the flocs, k'_A and k'_B are aggregation and breakup efficiency coefficients, and p and q are model parameters. Through a scaling argument, p is typically taken to be $p = 3 - n_f$ (Winterwerp, 1998; Kuprenas et al., 2018). And following the reasoning of Kuprenas et al. (2018) and set q to be a simple function of the size of the flocs relative to the Kolmogorov microscale, $\eta = \sqrt{G/\nu}$:

$$q = c_1 + c_2 \frac{d_{50}}{\eta} \tag{A4}$$

where c_1 and c_2 are constant coefficients. The proposed formulation ensures k_B increases as d_{50} approaches η.

For the fit to the Mississippi River data, we used the profile averaged measurements of d_50, concentration, and G; depth-averaged G was estimated from the data using $G = \sqrt{U u_*^2/(\nu H)}$. Water density and viscosity were set based on water temperature and salinity of zero. Other model coefficients used included: $d_p = 6$ μm, $\rho_s = 2650$ kg/m^3, $F_y = 10^{-10}$ N, $c_1 = 0.5$, $c_2 = 1.5$, and $n_f = 2$. Reasonable values for k'_A/k'_B needed to describe the data under these conditions were $k'_A/k'_B = 1.5 \times 10^5$ during summer and $k'_A/k'_B = 3.0 \times 10^4$ during winter. These ratios are used to produce the fit lines of Fig. 7.